CELL STRUCTURE AND FUNCTION 23: 73–84 (1998)
© 1998 by Japan Society for Cell Biology

Differential Distribution of Actin and Cytokeratin in Isolated Full-length Rabbit Renal Tubules

Kaori Goto* and Harunori Ishikawa

Department of Anatomy, Gunma University School of Medicine, Maebashi, Gunma 371–8511, Japan

Key words: renal tubule/Bowman's capsule/actin/cytokeratin/confocal microscopy/electron microscopy

ABSTRACT. **The distribution of basal actin bundles and cytokeratin intermediate filaments in the rabbit kidney was examined along isolated renal tubules by confocal laser microscopy. Perfusion of collagenase and subsequent manipulation of kidney tissues yielded well preserved renal tubules free of connective tissue components often extending from glomeruli to collecting tubules. Such isolated renal tubules were fluorescently stained with phalloidin and with anti-cytokeratin antibody and then observed as whole-mount preparations by confocal laser microscopy. Epithelial cells of Bowman's capsules showed conspicuous actin bundles which were arranged parallel to each other in individual cells. In proximal ducts, thick actin bundles were seen running in the basal regions of epithelial cells perpendicular to the tubule axis. Basal actin bundles in proximal tubules appeared to be somewhat thinner and run more irregularly in more distal parts of the tubule. Thin limbs of Henle's loop showed bright but very short rod or dot-like stainings of actin, while in thick limbs, there were thick and short actin bundles. In distal tubules basal actin bundles wre somewhat longer than those in thick limbs of Henle's loop. In the collecting ducts in the renal cortex, a few short actin bundles as well as dotty or patchy stainings were shown in the basal region. In both whole-mount preparations and cryostat sections, cytokeratin immunoreactivities were almost exclusively detected in epithelial cells of Henle's loops and collecting ducts but poorly in proximal and distal tubules. Epithelial cells of Henle's loops showed dense networks of cytokeratin immunoreactivities throughout the cytoplasm, whereas cell boundaries were immunostained in collecting ducts. The actin and cytokerating distribution in such isolated renal tubules was confirmed by immunofluorescence of cryostat sections and by thin-section electron microscopy. The observations that actin and intermediate filaments varied in distribution in different segments of renal tubules are interesting in view of the segmental differentiation of renal tubule functions.**

Actin is one of the most conserved and ubiquitous proteins in eukaryotic cells. Actin forms filaments as one of the major components of the cytoskeleton and is often distributed as bundles of actin filaments in a wide variety of tissue cells. Actin bundles are extensively developed in cultured cells and are traditionally known as stress fibers. The stress fiber is characterized by a parallel bundle of actin filaments with their bidirectional polarities, by codistribution of myosin, α-actinin and some other actin-binding proteins along its course, by anchorage on the plasma membrane, and by occurrence as a stationary structure within a limited time (5, 8, 14). In the stress fiber, various contractile proteins are often organized into repeated units, comparable to the sarcomeres in striated muscle myofibrils (31). Based on such criteria, stress fibers are also identified in various tissue cells (9, 27, 30, 33, 34, 39).

In the kidney, epithelial cells in proximal tubule possess prominent bundles of microfilament at the basal region (16, 25). Those microfilaments were identified as actin bundles (28, 29, 36) by the heavy meromyosin decoration method (15). The localization of actin in the kidney was also demonstrated by staining cryostat sections with fluorescentlylabeled phallotoxin (1). More recently, actin bundles in rat proximal tubules have been identified as stress fibers (23). The expression of intermediate filament proteins, another major component of the cytoskeleton, has been immunohistochemically detected in the kidney (12, 13, 17, 21, 26, 37, 38, 40), but that in epithelial cells of renal tubules has not drawn much attention. Moreover, the variation of the distribution patterns of actin and intermediate filaments in different segments of renal tubules, if any, has not been well documented.

In the present study, we tried to isolate full-length renal tubules from the rabbit kidney for confocal laser microscopy combined with whole-mount preparations. With this approach, we successfully documented the overall distribution of actin and intermediate filaments

* To whom correspondence should be addressed.
Tel: +81–272–20–7912, Fax: +81–272–20–7916

in three dimensions while clearly identifying each segment of the renal tubules.

MATERIALS AND METHOD

Isolation of Renal Tubules

White rabbits (Japanese strain) weighing around 1.8 kg were used in this study. The animal was anesthetized with sodium pentobarbital and the left kidney was perfused with 100 ml of a solution (pH 7.2) consisting of 0.5 mM EGTA, 0.137 M NaCl, 5.4 mM KCl, 0.5 mM NaH_2PO_4, 0.42 mM Na_2HPO_4, 1 mM N-2-hydroxyethylpiperazine-N′-2-ethanesulfonic acid (HEPES), 1 mM $NaHCO_3$, and 5 mM glucose, and subsequently with an enzyme solution (pH 7.5) consisting of 0.05% collagenase type IV (Sigma, St. Louis, MO USA), 0.005% trypsin inhibitor (Sigma), 0.137 M NaCl, 5.4 mM KCl, 5 mM $CaCl_2$, 0.5 mM NaH_2PO_4, 0.42 mM Na_2HPO_4, and 0.42 mM $NaHCO_3$. The solution was warmed to 37°C before perfusion (32). The kidney was excised just after perfusion, immersed in ice-cold Dulbecco's modified phosphate buffer saline (PBS), and carefully dissected to isolate renal tubules under a dissection microscopy. Such isolated tubules were washed in PBS and processed for microscopy.

Isolation of Bowman's Capsules

Bowman's capsules were isolated according to the method of Murakami and Ishikawa (23). In brief, the left kidneys of rabbits anesthetized and sacrificed by cervical bleeding were excised and immersed in ice-cold PBS. The renal cortex was cut into small pieces, gently homogenized by a teflon homogenizer, and then centrifuged to obtain tissue fragments including Bowman's capsules.

Fluorescence Staining

Isolated renal tubules and Bowman's capsules were fixed with 4% paraformaldehyde (PFA) in PBS for 30 min at room temperature, incubated with 1% Triton X-100 in PBS for 10 min, and then washed with PBS. For actin filaments, such fixed samples were stained with 0.17 mg/ml FITC-conjugated phalloidin (Sigma). For intermediate filaments, the samples were blocked with 10% normal goat serum (Biosource, Camarillo, CA USA) for 30 min at room temperature and treated overnight at 4°C with mouse monoclonal anti-cytokeratin cocktail (MAK-6, Zymed Laboratories Inc., South San Francisco, CA USA) diluted to 1:50 with 1% bovine serum albumin in PBS. The specimens were washed three times with PBS for 15 min each, treated with FITC- or Texas red-labeled goat antimouse IgG (E-Y Laboratories, San Mateo, CA USA) for 2 hr, and

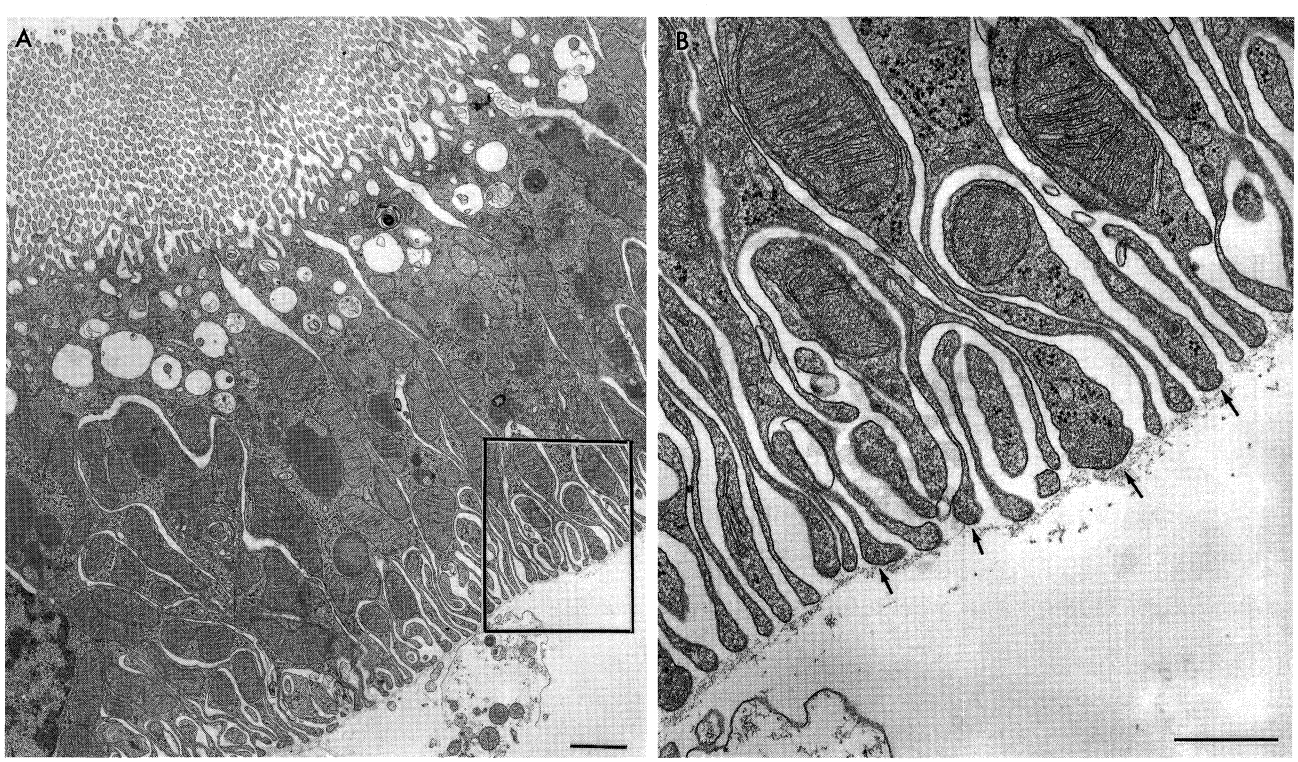


Fig. 1. Thin-section electron micrographs of the basal part of an isolated proximal tubule in cross-section. A: Connective tissue components around the tubule are removed almost completely with thin basement membrane remained. This method does not affect the overall ultrastructural integrity of the renal tubules. Bar, 1 μm. B: Enlarged image of part of Fig. 1A (square). Bundles of actin filaments appear to remain intact at the basal cytoplasm. Bar, 500 nm.

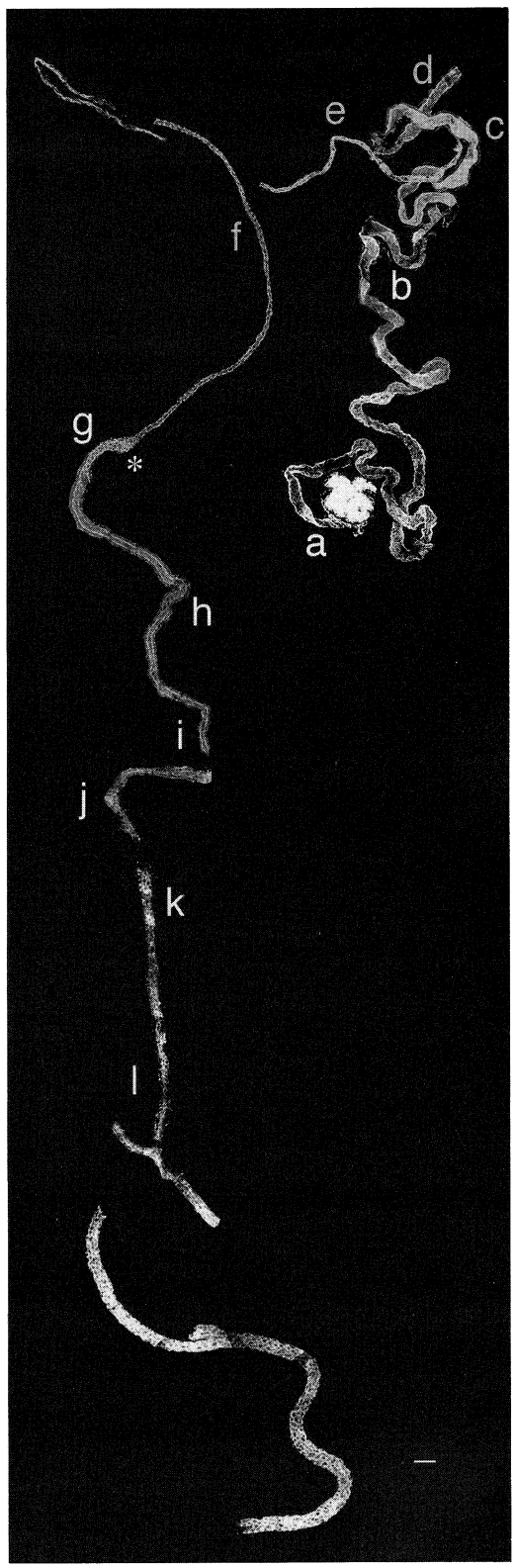


Fig. 2.

then washed in PBS. Cryostat sections were consecutively cut and stained with phalloidin for actin, with eosin-hematoxyline for structure, or histochemically for Na^+-K^- ATPase activity (19).

Confocal Laser Microscopy

Isolated renal tubules and Bowman's capsules were carefully spread on glass slides with a needle under a phase contrast microscope. The specimens were mounted in 2.5% 1,4-diazabicyclo (2.2.2)-octane (DABCO), 50% glycerol, and 20% Mowiol 4-48 (Calbiochem, La Jolla, CA USA), 0.2 M Tris-HCl, pH 8.5 and examined with an MRC-600 confocal laser microscope (Bio-Rad, Cambridge, UK) mounted on a Zeiss Axiophot microscope.

Electron Microscopy

For electron microscopy, isolated renal tubules and Bowman's capsules were fixed with 2% PFA-2.5% glutaraldehyde in 0.1 M sodium cacodylate buffer, pH 7.3, for 1 hr at room temperature and then with 1% osmium tetroxide in the same buffer for 1 hr at 4°C. Such fixed samples were processed by routine procedures for thin-section electron microscopy. Thin sections were cut and examined with a Hitachi H-800 electron microscope.

Western Blot Analysis

Fresh renal cortex and medulla were separately homogenized in cold PBS containing 1% phenylmethylsulfonylfluoride (PMSF), suspended in sodium dodecyl sulfate (SDS) sample buffer, boiled and then centrifuged. The supernatant was electrophoresed in 10% acrylamide slab gel according to Laemmli's method. The electrophoresed proteins were transferred onto Immobilon-P membrane (Millipore, Bedford, USA). The membranes were incubated with anti-cytokeratin, treated with horseradish peroxidase-conjugated goat anti-mouse IgG (ICN Pharmaceuticals Inc., Costa Mesa, CA USA), and then visualized by ECL kit (Amersham, Buckinghamshire, UK) and 3-3′-diaminobenzidine tetrahydrocholoride (DAB) (Wako, Osaka, Japan).

RESULTS

Distribution of Actin in Isolated Renal Tubules

In an effort to isolate renal tubules for confocal microscopy of whole-mount preparations, we successfully applied collagenase digestion and microdissection to

Fig. 2. Confocal laser micrograph of an isolated renal tubule of full-length stained with FITC-phalloidin. Through-focus confocal images of each part were projected and combined to make a montage image of the whole tubule. Proximal tubule (a, b, c, d), Henle's loop (e, f), distal tubule (g, h, i) and collecting duct (j, k, l) are clearly seen. The macula densa (asterisk) can be identified by bulging of tubule with a plaque of cell aggregates at the beginning segment of the distal tubule. Breakage occurred at several points while mounting the tubule on a slide glass. Bar, 50 μm.

produce full-length tubules free of connective tissue components, not affecting the overall ultrastructural integrity of epithelial cells of the renal tubules as confirmed by thin-section electron microscopy (Fig. 1). In such isolated preparations, each segment of the tubule could be easily identified based on the distance from the glomerulus, the size of tubules, and the positional relationship between neighboring segments. The identification of renal segments was further confirmed by phalloidin staining, hematoxyline-eosin staining and Na^+-K^+ ATPase histochemistry in consecutive cryostat sections made from the same isolated tubules. We scanned favorable preparations of full-length renal tubules stained with FITC-phalloidin starting from the glomerulus to the collecting tubule with a confocal laser microscope to make montage images (Fig. 2). Reconstructed through-focus images were made from scanned sections of the basal part of the tubule to reveal the basal actin bundles eliminating fluorescent staining in other parts of the cells, especially brush borders.

The staining pattern of actin filaments varied in different segments of the tubule. Epithelial cells of Bowman's capsule showed conspicuous actin bundles in their flattened cytoplasm (Fig. 3). Actin bundles were long and thick and arranged parallel to each other or in a fan-like fashion. Some bundles appeared to have branchings to form a V- or Y-shape. It was estimated that individual cells have about 10 bundles, and that the length and width of bundles are 15.74 μm and 1.06 μm in average, respectively. The direction of actin bundles in a cell appeared to be unrelated to that in neighboring cells, and the actin bundles rarely extended to the cell-to-cell junctions to show continuous staining to the next cell.

The proximal tubule was characterized by bright phalloidin staining in basal actin bundles as well as at the brush border. Such basal actin bundles ran perpendicular to the tubule axis as previously described (23) (Fig. 4A, B). Basal actin bundles in the proximal tubule up to the Henle's loop appeared to be somewhat thinner and run more irregularly in more distal parts of the tubule. The average length and width of actin bundles were 2.83μm and 0.49 μm in the proximal part of the proximal tubule, and 2.12 μm and 0.29 μm in the distal part, respectively.

The thin limb of Henle's loop showed bright but very

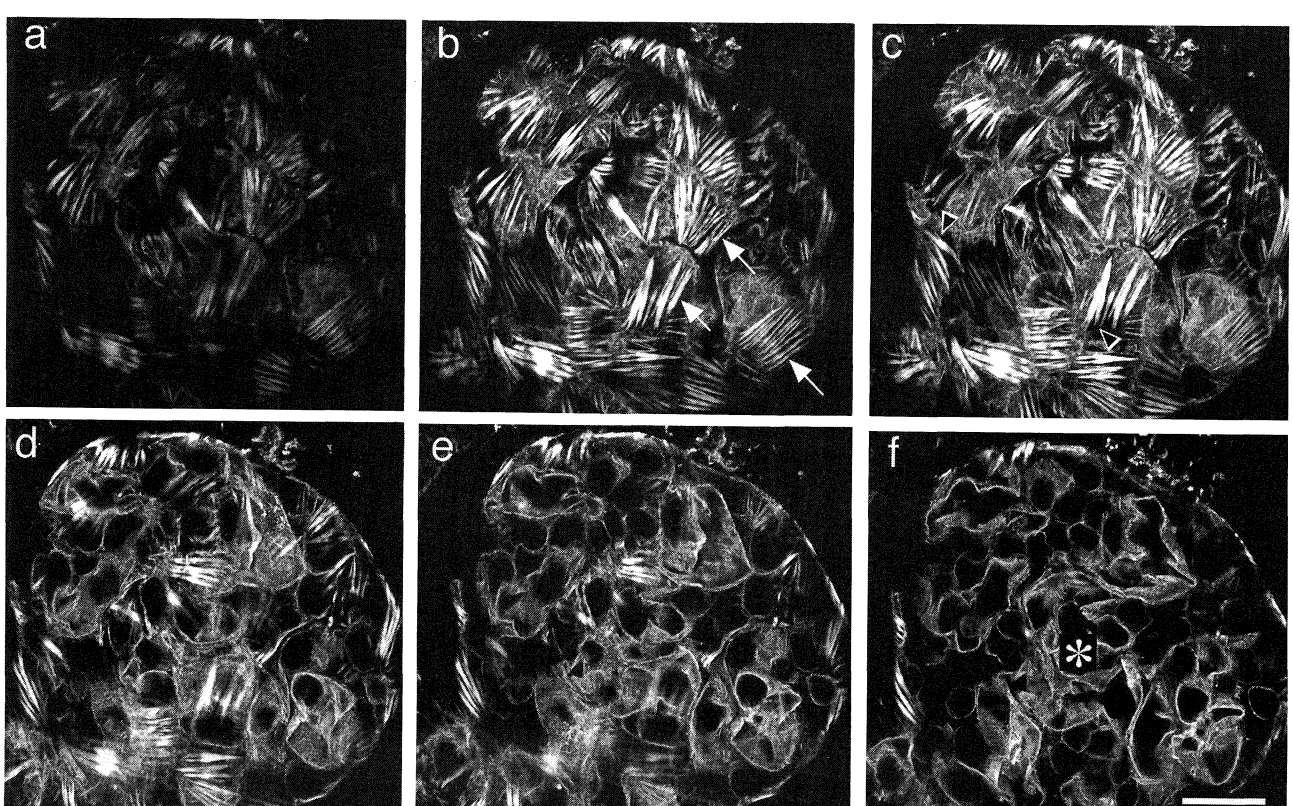


Fig. 3. Confocal laser micrographs of an isolated Bowman's capsule covering the glomerulus stained with FITC-phalloidin. Serial optical sections of 2 μm thickness were made from the outside surface (a) toward the glomerulus (f). Actin bundles (arrows) are arranged in parallel in individual cells, occasionally showing branchings (arrowheads). Asterisk; glomerulus. Bar, 25 μm.

short rod or dot-like stainings, most of which were less than 0.98 μm in length (Fig. 4C). In the basal part of the thick limb, there were thick and short actin bundles (mean values; 0.90 μm in length, 0.60 μm in width) in a background of dot-like, patchy or reticular patterns of staining (Fig. 4D). In serial optical sections, many of the dot-like or patchy stainings in Henle's loop appeared to be continuous with those in the next sections

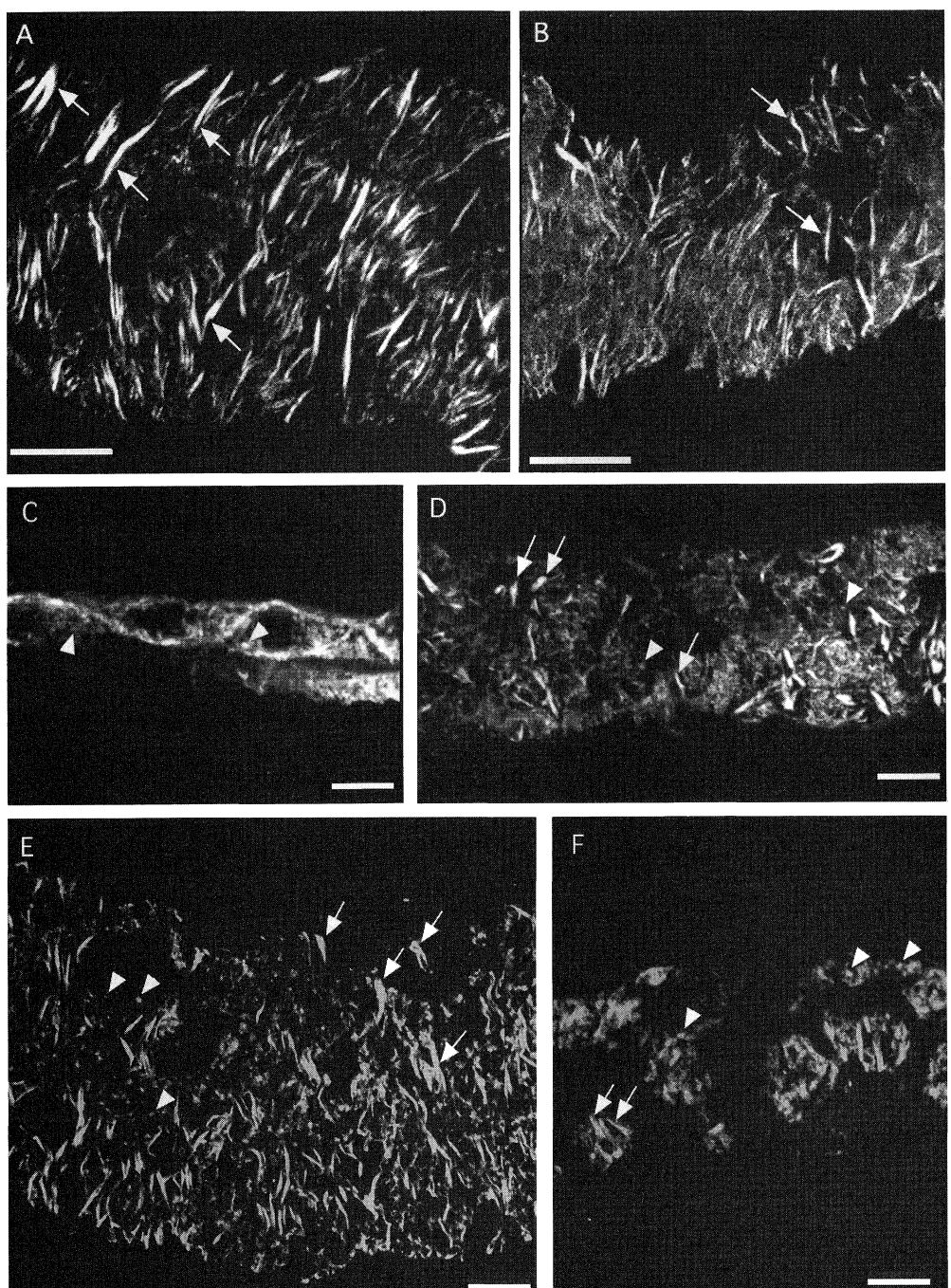


Fig. 4. Confocal laser micrographs of an isolated renal tubule stained with FITC-phalloidin. Serial optical sections of 1 μm thickness were made longitudinal to the tubule axis and projected in single images ranging from the outermost plane to the luminal surface. A, Part of the proximal tubule near Bowman's capsule. B, Part of the proximal tubule just before Henle's loop. C, thin limb of Henle's loop. D, thick limb of Henle's loop. E, Distal tubule. F, Collecting duct. Arrows indicate actin bundles. Arrowheads, dot-like staining of actin. Bars, 10 μm.

often following along the basal infolding (data not shown). The basal actin bundles did not appear to run in a certain direction.

Phalloidin staining in the distal tubule revealed actin bundles in a background of reticular patterns of staining in the basal region as those found in Henle's loop, though actin bundles in the distal tubule were somewhat longer than those in Henle's loop (Fig. 4E). The length and width of actin bundles were 1.21 μm and 0.53 μm on average, respectively. Many of the bundles ran nearly perpendicular to the tubule axis.

There were dense networks of actin bundles in the basal region of the macula densa (usually situated in the final segments of the thick limb of Henle's loop in the rabbit kidney). The basal part of cell and lateral surface were also positive in phalloidin staining (Fig. 5).

In the collecting ducts in the renal cortex, there were a few short actin bundles as well as dotty or patchy stainings in the basal region (mean values: 1.71 μm in length, 0.79 μm in width). The direction of actin bundles appeared to be random as in Henle's loops (Fig. 4F).

The relative values of the mean fluorescence intensity of the phalloidin-stained actin bundles in Bowman's capsule, proximal tubule, thin limb of Henle's loop,

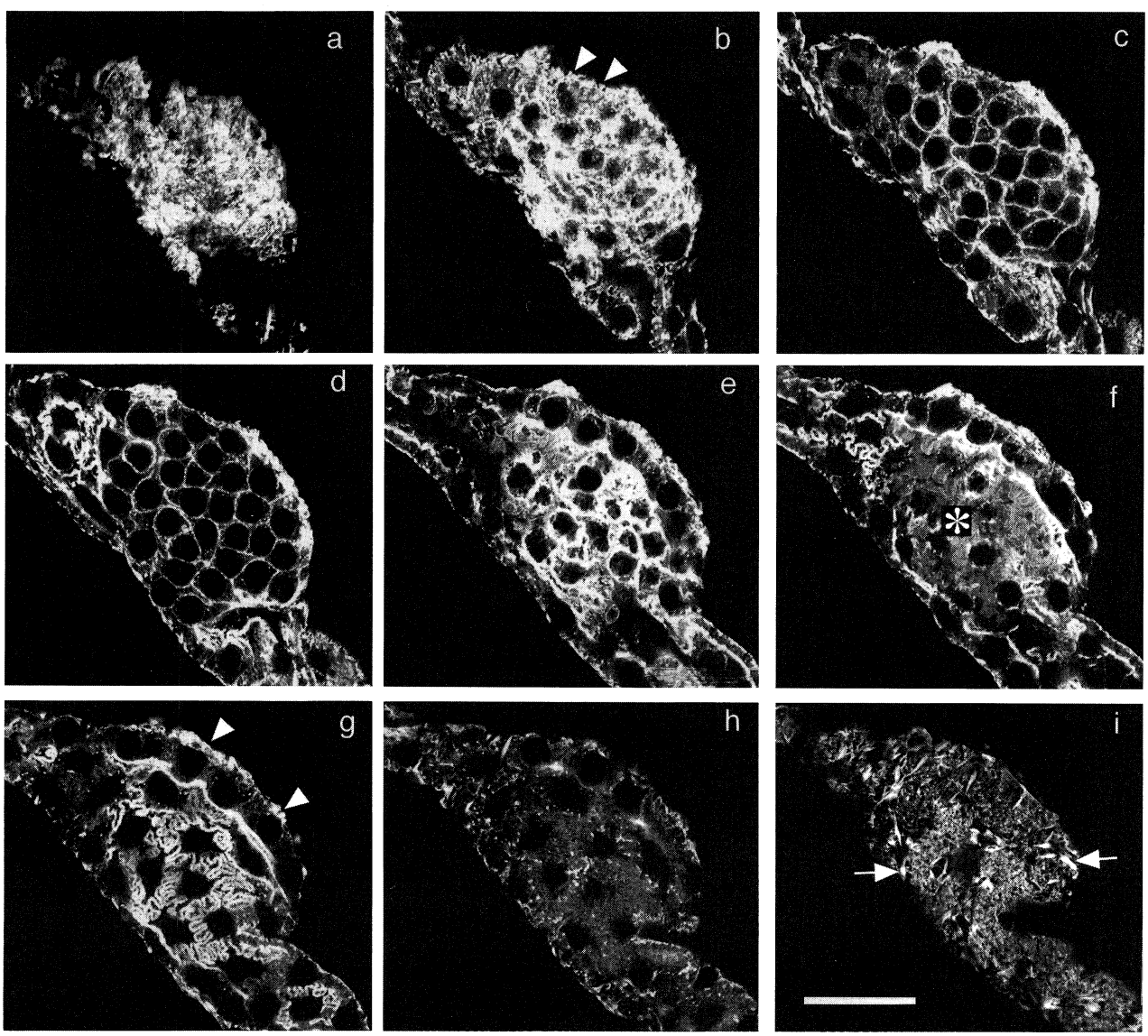


Fig. 5. Confocal laser micrographs of a macula densa stained with FITC-labeled phalloidin. Serial optical sections (a–i) were made longitudinal to the tubule axis ranging from the outside surface of the macula densa (a) to the other side of the tubule (f). Note actin staining in the macula densa (arrowhead), and actin bundles on the other side of the tubule (arrow). Asterisk indicates the lumen of tubules. Bar, 25 μm.

thick limb of Henle's loop, distal tubule and collecting duct were 0.66:1:1:0.36:0.66:1, respectively.

The distribution of basal actin bundles in different parts of the renal tubules was quantified by such parameters measured in reconstructed images of the basal part of the tubules as the sum of apparent area of individual actin staining, the number of bundles, and the direction of bundles relative to the tubular axis, as summarized in Fig. 6. We excluded dot-like and patchy stainings in this estimation. The results, as the proximal and distal tubules had higher values of phalloidin staining in area than other segments of the tubules, but that the number of actin stainings was virtually the same between the proximal tubule and Henle's loop. Many of the actin bundles ran more or less perpendicular to the tubule axis in the proximal and distal tubules, while the directions of actin bundles were rather random in other segments.

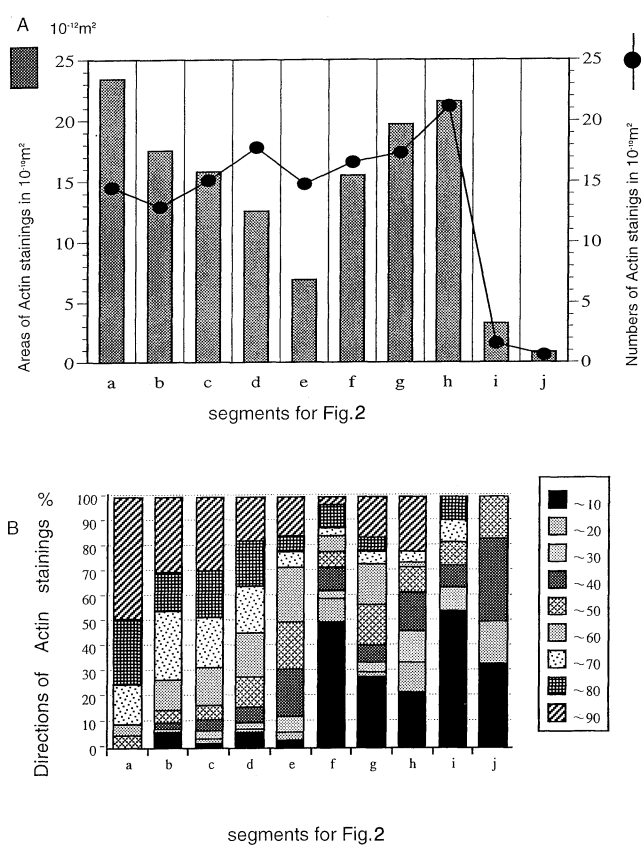


Fig. 6. Morphometry of basal actin bundles in an isolated tubule. Measurements were made on the same tubule shown in the Fig. 2. Alphabets on the horizontal axis also correspond to those in Fig. 2. A, Areas and numbers of basal actin stainings per 10^{-10} m^2 measured in reconstructed images of renal tubule. B, Directions of basal actin bundles relative to the tubule axis.

Distribution of Actin in Interstitial Cells

To answer the question if the observed difference in actin distribution in epithelial cells of the renal tubules may be related to other components, especially the interstitial connective tissue, cryostat sections were stained with fluorescent phalloidin for confocal microscopy. The observation showed that in the renal medulla interstitial cells around collecting ducts had well-developed actin bundles which ran perpendicular to the tubule axis

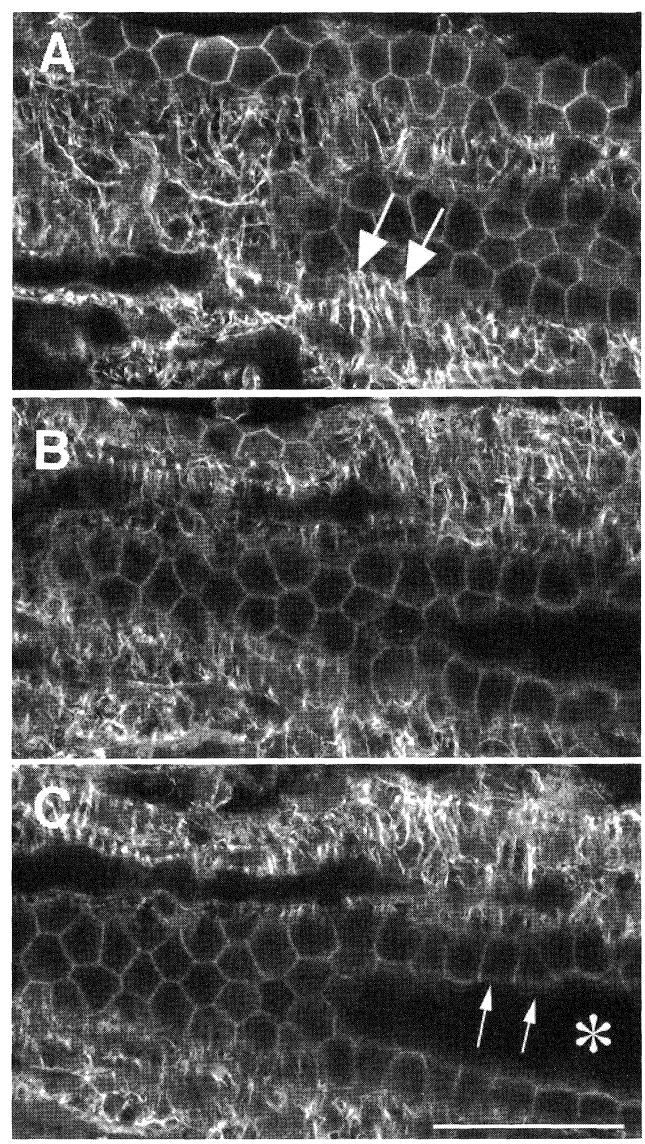


Fig. 7. Confocal micrograph of a collecting duct in a cryostat section stained with FITC-phalloidin. Serial optical sections of 4 μm thick were made longitudinal to the tubule. Actin staining is seen along the cell surface and boundary (small arrows) in collecting duct epithelial cells. Interstitial cells around the collecting duct show prominent actin bundles running perpendicular to the tubule axis (large arrows). Asterisk, lumen. Bar, 50 μm.

(Fig. 7). The collecting ducts themselves contained much fewer actin bundles at the basal regions of the epithelial cells. Interestingly, there were few, if any, interstitial cells in the renal cortex and actin bundles in those cells showed no regular arrangement (data not shown).

Distribution of Cytokeratin in Isolated Renal Tubules

Isolated segments of renal tubules were stained with anti-cytokeratin antibody and examined by confocal laser microscopy. Henle's loops, particularly their thin limbs, and the medullar part of collecting ducts showed strong immunoreactivities, while Bowman's capsules and the proximal and the distal tubules had faint reactivities (Fig. 8A). Similar results were obtained from anti-cytokeratin staining of cryostat sections. The spotty staining in the proximal tubule was also found in negative controls without the primary antibody, suggesting that this may represent a cross-reactivity of the secondary antibody with the intrinsic immunoglobulins engulfed in the cytoplasm.

In Henle's loops, reticular staining patterns which were particularly strong along the tubular lumen (Fig. 8B). Thin-section electron microscopy showed networks of intermediate filaments in the epithelial cells of the Henle's loop (Fig. 9). The collecting ducts in the renal medulla also showed reticular staining patterns throughout the cytoplasm but these patterns were remarkably stronger along the cell boundary (Fig. 8C). The collecting ducts in the renal cortex showed only faint immunoreactivities.

Likewise, immunoblotting for cytokeratin showed a thick band of 45 kDa in samples from the renal medulla and a faint band in those from the superficial part of the renal cortex (Fig. 10).

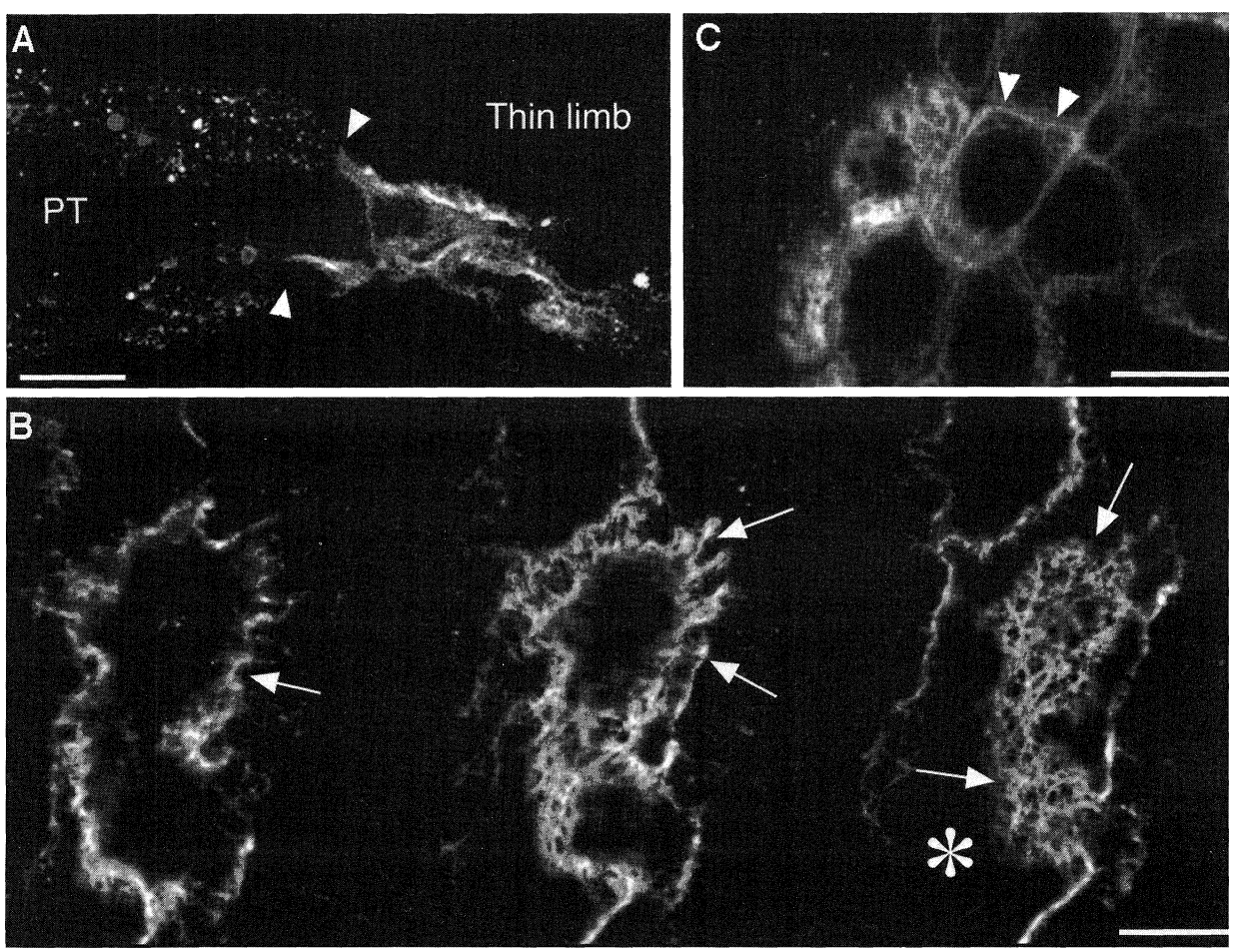


Fig. 8. Confocal laser micrograph of a isolated tubule stained with anti-cytokeratin. A, Reconstructed image of the transitional part (large arrowheads) between the proximal tubule and the thin limb of Henle's loop. Cytokeratin immunoreactivity is strongly positive in the thin limb. Note spotty stainings in the cytoplasm of the proximal tubule. B, Serial optical sections of the thick limb of Henle's loop with 1 μm/step. Arrows indicate reticular pattern of cytokeratin staining on the luminal surface of the tubule. Asterisk, lumen. C, An optical sections of the collecting duct. The reticular pattern of cytokeratin staining is seen along the cell boundary (arrowheads). Bars, 10 μm.

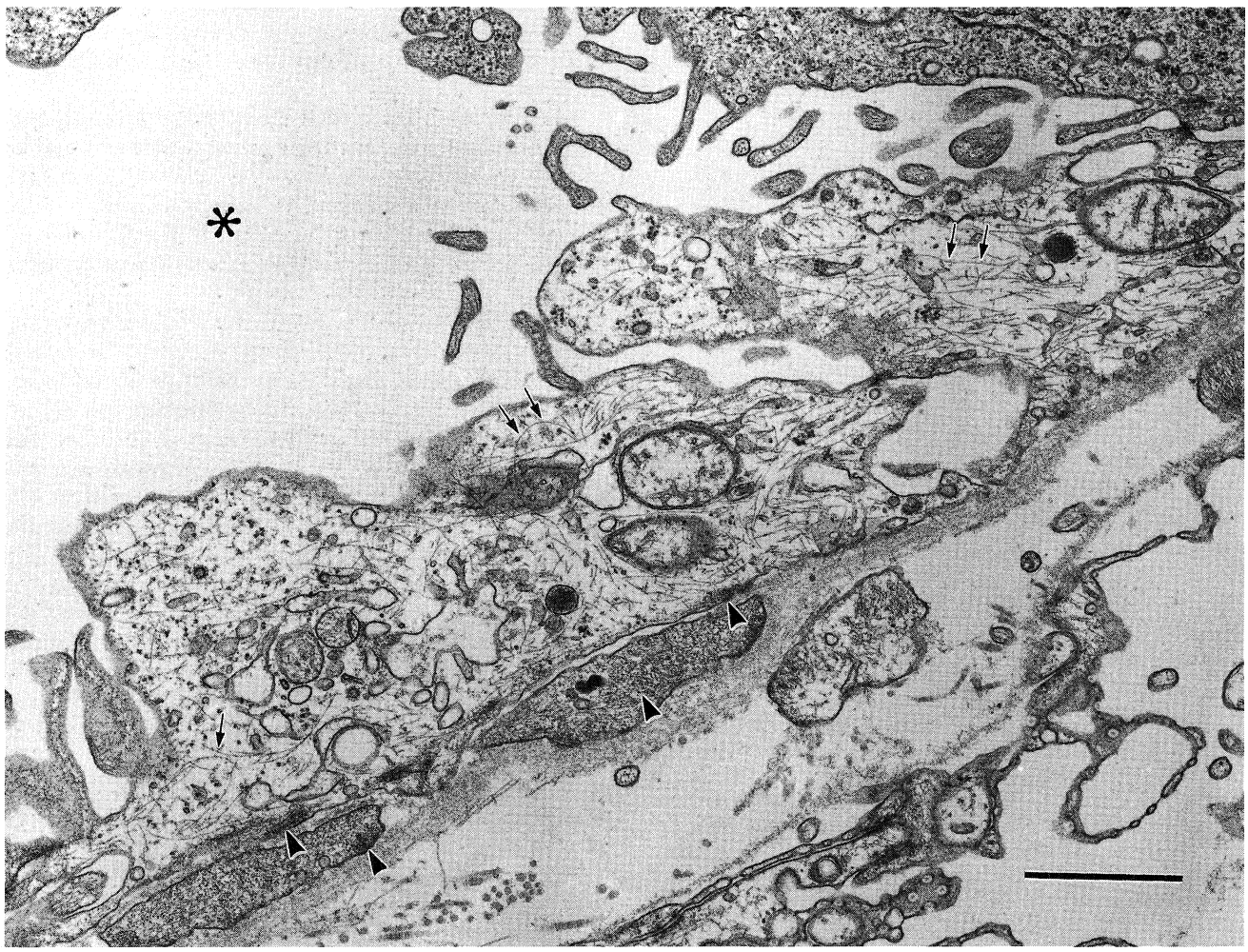


Fig. 9. Thin-section electron micrograph of the thin limb of Henle's loop. Intermediate filaments (arrow) are seen throughout the cytoplasm of epithelial cells at the initial part of the thin limb of Henle's loop. Actin bundles (arrowheads) are seen on the basal region of the epithelial cells. Asterisk, lumen. Bar, 1 μm.

DISCUSSION

Many studies have documented the distribution of cytoskeletal components in Bowman's capsules and renal tubules by electron microscopy (16, 25, 28, 29, 36), immunohistochemistry (12, 13, 17, 21, 26, 37, 38, 40), and flurorescence microscopy (1, 23). However, the observations have been limited to certain segments of the nephron leaving overall distributions undefined. In the present study, we have taken advantage of confocal laser microscopy combined with whole-mount preparations of isolated renal tubules to successfully reveal the overall distribution of actin and intermediate filaments in well identified segments. For this purpose, we employed the digestion method to the rabbit kidney tissue followed by microscopic manipulation to isolate continuous renal tubules.

The isolation procedure used allowed us to we used preserve relatively well the overall ultrastructural integrity of epithelial cells of the renal tubules. The enzyme solution was widely used as Seglen's solution for hepatocyte primary culture. We tested another enzyme solution (collagenase in Hank's solution), but the ultrastructural integrity of epithelial cells was not better preserved than that with Seglen's enzyme solution.

The distribution pattern of actin and cytokeratin intermediate filaments varied in different segments of renal tubules. The distribution pattern of actin filaments in certain renal tubules were consistent with previously reported findings (1, 16, 23, 25, 28, 29, 36). In our study, the intermediate filaments were not shown to be present in Bowman's capsule, proximal tubule and distal tubule, where cytokeratin was positively stained in previous investigations (26). This discrepancy may be at-

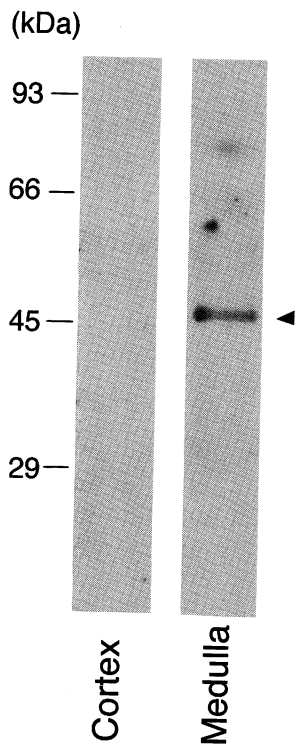


Fig. 10. Immunoblotting for cytokeratin. Glycerol-extracted samples from the renal cortex and medulla were electrophoresed in a slab gel, transferred onto a nitrocellulose membrane, and stained with an anti-cytokeratin antibody. Total proteins loaded were approximately 1 mg/lane. A prominent band at 45 kD is seen in the sample of the medulla, whereas the corresponding band is not detected in the sample of the cortex. Numbers on the left indicate the molecular weights of marker proteins in kD.

tributed to different antibodies used or to the species difference of animals examined.

Such variations may be related to the functional differences of segments of renal tubules. Hence, it is interesting to correlate the distribution pattern of actin and intermediate filaments to morphological and physiological conditions of different segments of renal tubules. In the present study, the areas of confocal images of fluorescently stained actin bundles were measured as a convenient parameter of actin development. Some factors such as hydraulic pressure, flow rate and shear stress can conceivably account for the observed differences. Thus, those factors may act differently in different segments of the renal tubules.

In Bowman's capsules, actin bundles were highly developed showing thick and long bundles. Actin bundles were arranged in a parallel or fan-like fashion within individual epithelial cells, but not connected to those of neighboring cells. Since Bowman's capsule is considered to serve as a transient container for the glomerular filtrate before entering the proximal tubule, the epithelial cells may be subject to high hydraulic pressure caused by the filtrate. Thus, it is interesting to speculate that actin bundles may develop this distribution pattern to maintain their shape and position against such mechanical forces.

In proximal tubules, actin filaments are arranged into bundles running at right angle to the tubule axis and attaching to the basal plasma membrane with both their ends to form stress fibers (23). Such basal actin bundles may serve to reinforce the attachment of cells to the extracellular matrix rather than to actively constrict the tubules.

Basal actin bundles in the proximal tubule were thinner and shorter in more distal segments. It is well known that water and sodium chloride in urine are most effectively reabsorbed in proximal tubules (20). As urine passes along the tubules, water is absorbed and the volume of flux and the hydraulic pressure decrease gradually. Indeed, the hydraulic pressure in the rat kidney that averages $12.5+2.2$ mmHg in proximal tubules may be as low as 6.7 ± 1.6 mmHg in distal tubules (10, 11). Likewise, micropuncture studies with cats showed that the capillary pressure in glomeruli was 62.6 ± 1.4 mmHg and the hydraulic pressure in proximal tubules was 19.8 ± 1.1 mmHg (4). It seems that the development of actin bundles is proportional to the hydraulic pressure in the tubule lumen. Since the renal segment with most complex basal infoldings is the proximal tubule, such ultrastructural specializations seem to be maintained against high hydraulic pressure by developed basal actin bundles.

In Henle's loops, basal actin bundles were thin and short, while cytokeratin staining is conspicuously strong. As compared to the proximal tubules, the caliber of Henle's loops is much smaller such that the flow rate is much faster and the lateral pressure exerted on the epithelium may be higher. On the other hand, the shear stress is inversely proportional with 3 involutions to the radius in the tubule lumen (2, 6, 7, 18, 22). Such physical characteristics may reflect the observed distribution pattern of cytoskeletal components, though their correlation is difficult. It is also conceivable that abundant cytokeratin filaments seem to compensate for poorly developed actin bundles in Henle's loops.

In collecting ducts, basal actin bundles were poorly developed as compared to other segments of renal tubules. As 98% of the water of the original glomerular filtrate is absorbed before reaching the collecting ducts (35), the hydraulic pressure and shear stress to collecting duct cells are considered to be very low. It is interesting to note that epithelial cells of the collecting duct appear to be well contoured with cuboidal cell shape without elaborate interdigitation of the apposed lateral cell membranes. Moreover, both actin and cytokeratin filaments were distributed along the cell boundary. This suggests that actin and cytokeratin filaments may func-

tion to maintain the cell shape by reinforcing clel junctions and boundaries.

Interestingly, actin bundles were rich in interstitial cells around or between collecting ducts in the renal medulla but not so conspicuous in the cortex. Bundles of actin filaments in the interstitial cells have been observed by thin-section electron microscopy (3, 24). The present study has clearly demonstrated the overall distribution of actin bundles in interstitial cells. Such limited distribution of actin filaments prompts us to speculate that they may reinforce the structural integrity of collecting ducts from outside. Thus, the basal actin bundles and cytokeratin filaments may be formed to accommodate renal tubules to their local physiological conditions.

Acknowledgements. This work was supported in part by a Grants-in-Aid for Scientific Research from the Ministry of Education, Science, and Culture of Japan. We are very grateful to Dr. T. Murakami for his helpful discussion and critical reading of the manuscript, to Dr. T. Hijikata for guidance in Western blot analysis technique, to Dr. O. Shimada for guidance in immunohistochemistry technique, and to Dr. N. Fujimaki for encouragement throughout this work.

REFERENCES

1. Andrews, P.M. and Bates, S.B. 1984. Filamentous actin bundles in the kidney. *Anat. Rec.,* **210**: 1–9.
2. Bhat, V.D., Windridge, P.A., Cherry, R.S., and Mandel, L.J. 1995. Fluctuating shear stress effects on stress effects on stress fiber architecture and energy metabolism of cultured renal cells. *Biotechnol. Prog.,* **11**: 596–600.
3. Bohman, S.-O. and Jensen, P.K.A. 1976. Morphometric studies on the lipid droplets of the interstitial cells of the renal medulla in different states of diuresis. *J. Ultrastruct. Res.,* **55**: 182–192.
4. Brown, S.A. and Brown, C.A. 1995. Single-nephron adaptations to partial renal ablation in cats. *Am. J. Physiol.,* **269**: R1002–R1008.
5. Byers, H.R., White, G.E., and Fujiwara, K. 1984. Organization and function of stress fibers in vitro and in situ. In *Cell and Muscle Motility, Vol.5* (J.W. Shay, ed.). Plenum Press, New York, pp.83–137.
6. Cucina, A., Sterpetti, A.V., Pupelis, G., Fragale, A., Lepidi, S., Cavallaro, A., Giustiniani, Q., and D'Angelo, L.S. 1995. Shear stress induces changes in the morphology and cytoskeleton organization of arterial endothelial cells. *Eur. J. Vasc. Endovasc. Surg.,* **9**: 86–92.
7. Davies, P.F., Remuzzi, A., Gordon, E.J., Dewey, C.F. Jr., and Gimbrone, M.A.Jr. 1986. Turbulent fluid shear stress induces vascular endothelial cell turnover in vitro. *Proc. Natl. Acad. Sci. USA,* **83**: 2114–2117.
8. Fujiwara, K., White, G.E., and White, L.D. 1985. Role of in situ stress fibers in cellular adhesion. In *Cell Motility: Mechanism and Regulation* (H. Ishikawa, S. Hatano and H. Sato, eds.). University of Tokyo Press, Tokyo, pp.477–492.
9. Furumura, M. and Ishikawa, H. 1996. Actin bundles in human hair follicles as revealed by confocal laser microscopy. *Cell Tissue Res.,* **283**: 425–434.
10. Gottschalk, C.W. and Mylle, M. 1956. Micropuncture study of pressures in proximal tubules and peritubular capillaries of the rat kidney and their relation to ureteral and renal venous pressures. *Am. J. Physiol.,* **185**: 430–439.
11. Gottschalk, C.W. and Mylle, M. 1957. Micropuncture study of pressures in proximal and distal tubules and peritubular capillaries of the rat kidney during osmotic diuresis. *Am. J. Physiol.,* **189**: 323–328.
12. Holthöfer, H., Miettinen, A., Lehto, V.-P., Lehtonen, E., and Virtanen, I. 1984. Expression of vimentin and cytokeratin types of intermediate filament proteins in developing and adult human kidneys. *Lab. Invest.,* **50**: 552–559.
13. Howie, A.J. and Johnson, G.D. 1992. Confocal microscopic and other observations on the distal end of the thick limb of the human loop of Henle. *Cell Tissue Res.,* **267**: 11–16.
14. Ishikawa, H. 1985. Ultrastructural organization of the stress fiber. In *Cell Motility: Mechanism and Regulation* (H. Ishikawa, S. Hatano and H. Sato, eds.). University of Tokyo Press, Tokyo, pp.451–460.
15. Ishikawa, H., Bischoff, R., and Holtzer, H. 1969. Formation of arrowhead complexes with heavy meromyosin in a variety of cell types. *J. Cell Biol.,* **43**: 312–328.
16. Kaissling, B. and Kriz, W. 1979. Structural analysis of the rabbit kidney. In *Advances in Anatomy, Embryology and Cell Biology, Vol.56* (A. Brodal, W. Hild, J. van Limbrogh, R. Ortmann, T.H. Schiebler, G. Töndury and E. Wolff, eds.). Springer-Verlag, Berlin, pp.42–51.
17. Kloth, S., Aigner, J., Brandt, E., Moll, R., and Minuth, W.W. 1993. Histochemical markers reveal an unexpected heterogeneous composition of the renal embryonic collecting duct epithelium. *Kidney Int.,* **44**: 527–536.
18. Malek, A.M. and Izumo, S. 1996. Mechanism of endothelial cell shape change and cytoskeletal remodeling in response to fluid shear stress. *J. Cell Sci.,* **109**: 713–726.
19. Mayahara, H., Saito, T., Hirano, H., and Ogawa, K. 1967. The new lead citrate method for the ultracytochemical demonstration of activity of non-specific alkaline phosphatase (orthophosphoric monoester phosphohydrolase). *Histochemie,* **11**: 88–96.
20. Mercer, P.F., Maddox, D.A., and Brenner, B.M. 1974. Current concepts of sodium chloride and water transport by the mammalian nephron. *West. J. Med.,* **120**: 33–45.
21. Moll, R., Hage, C., and Thoenes, W. 1991. Expression of intermediate filament proteins in fetal and adult human kidney: modulations of intermediate filament patterns during development and in damaged tissue. *Lab. Invest.,* **65**: 74–86.
22. Morita, T., Kurihara, H., Maemura, K., Yoshizumi, M., Nagai, R., and Yazaki, Y. 1994. Role of Ca^{2+} and protein kinase C in shear stress-induced actin depolymerization and endothelin 1 gene expression. *Circ. Res.,* **75**: 630–636.
23. Murakami, T. and Ishikawa, H. 1991. Stress fibers in situ in proximal tubules of the rat kidney. *Cell Struct. Funct.,* **16**: 231–240.
24. Newstead, J.D. 1971. Filaments in renal parenchymal and interstitial cells. *J. Ultrastruct. Res.,* **34**: 316–328.
25. Olsen, T.S., Olsen, H.S., and Hansen, H.E. 1984. Hypertrophy of actin bundles in tubular cells in acute renal failure. *Ultrastruct. Pathol.,* **7**: 241–250.
26. Oosterwijk, E., Van muijen, G.N.P., Oosterwijk-Wakka, J.C., and Warnaar, S.O. 1990. Expression of intermediate-sized filaments in developing and adult human kidney and in renal cell carcinoma. *J. Histochem. Cytochem.,* **38**: 385–392.
27. Petroll, W.M., Cavanagh, H.D., Barry, P., Andrews, P.,

and JESTER, V. 1993. Quantitative analysis of stress fiber orientation during corneal wound contraction. *J. Cell Sci.*, **104**: 353–363.

28. ROSS, M.H. and REITH, E.J. 1970. Myoid elements in the mammalian nephron and their relationship to other specializations in the basal part of kidney tubule cells. *Am. J. Anat.*, **129**: 399–416.
29. ROSTGAARD, J., KRISTENSEN, B.I., and NIELSEN, L.E. 1972. Electron microscopy of filaments in the basal part of rat kidney tubule cells, and their in situ interaction with heavy meromyosin. *Z. Zellforsch.*, **132**: 497–521.
30. SAGO, H., SUGIMOTO, K., FUJII, S., IINUMA, KI., YAMASHITA, K., KITAGAWA, M., and TERASHIMA, Y. 1993. Dynamic changes in stress fiber expression in rat uterine vein endothelial cells associated with pregnancy. *Microvasc. Res.*, **46**: 178–189.
31. SANGER, J.W. 1975. Intercellular localization of actin with fluorescently labelled heavy meromyosin. *Cell Tissue. Res.*, **161**: 431–434.
32. SEGLEN, P.O. 1976. Preparation of isolated rat liver cells. *Method Cell Biol.*, **13**: 29–83.
33. SUGIMOTO, K., FUJII, S., and YAMASHITA, K. 1991. Expression of stress fibers in bullfrog mesothelial cells in response to tension. *Exp. Cell Res.*, **196**: 353–361.
34. SUGIMOTO, K., YOSHIDA, K., FUJII, S., TAKEMASA, T., SAGO, H., and YAMASHITA, K. 1995. Heterogeneous responsiveness of the in situ rat vascular endothelial cells to mechanical stretching in vitro. *Eur. J. Cell Biol.*, **68**: 70–77.
35. SULLIVAN, L.P., WELLING, D.J., and ROME, L.A. 1981. Effects of sodium and chloride on potassium transport by the bullfrog kidney. *Am. J. Physiol.*, **240**: 127–137.
36. TANAKA, K., SHIBATA, N., and TATSUMI, N. 1977. Electron microscopic studies on the myofibrils in the epithelial cells of the Bowman's capsule and of proximal tubules in rat renal cortex. *Jap. Circ. J.*, **41**: 1329–1336.
37. VILAFRANCA, M. and FERRER, L. 1995. Ultrastructural co-localization of vimentin and cytokeratin in visceral glomerular epithelial cells of dogs with glomerulonephritis. *Res. Vet. Sci.*, **59**: 87–91.
38. WALDHERR, R. and SCHWECHHEIMER, K. 1985. Co-expression of cytokeratin and vimentin intermediate-sized filaments in renal cell carcinomas. *Virchows Arch. A Pathol. Anat. Histopathol.*, **408**: 15–27.
39. WHITE, G.E., GIMBRONE, M.A., and FUJIWATARA, K. 1983. Factors influencing the expression of stress fibers in vascular endothelial cells in situ. *J. Cell Biol.*, **97**: 416–424.
40. ZAITSEV, V.B. 1992. Cytoskeleton of podocytes in vertebrate animals and human. *Cell Mol. Biol.*, **38**: 823–833.

(Received for publication, January 25, 1998
and in revised form March 2, 1998)